High Heat Input Welding of Offshore Structures — Procedures and Weld Properties

With the right procedures, low-temperature impact properties can be retained with high heat input submerged arc welding

BY G. RØRVIK, M. I. ONSØIEN, A. O. KLUKEN AND O. M. AKSELSEN

ABSTRACT. In the present investigation, the properties of high heat input (E > 3 kJ/mm) deposited weld metals have been assessed, including nondestructive evaluation, side bend testing, hardness measurements, tensile, impact (Charpy V-notch) and fracture toughness (CTOD) testing. In addition, metallographic analyses were performed, using optical and scanning and transmission electron microscopy. The results obtained indicate that the weld properties do not represent a limiting factor when it comes to the application of high heat input flux cored and submerged arc welding, provided the formation of sufficient amounts of acicular ferrite. In this situation, both the Charpy V-notch impact energy and the CTOD fracture toughness satisfy the minimum levels required in current offshore specifications. However, in the case of high titanium (> 0.015 wt-% Ti) containing consumables, low weld metal Charpy V-notch and CTOD fracture toughness may occur after PWHT.

Introduction

For many years the heat input in welding of offshore structures has been limited to a maximum of 3 to 4 kJ/mm, because of the imminent risk of brittle fracture initiation within the weld metal and the grain coarsened heat-affected zone (HAZ). This is due to an expected formation of unfavorable microstructures, such as the coarse ferrite sideplates and the grain boundary ferrite, as a result of the slow cooling rates involved. However, recent developments in welding consumables and steelmaking practice, based on the philosophy of controlling transformation behavior through formation of finely dispersed nonmetallic inclusions (Refs. 1–4), have provided materials with a cleavage resistance less dependent on the weld heat input. Under such conditions, very fine grains of predominantly acicular ferrite (typical grain size of 1–3 μm) may form, resulting in excellent impact properties. Based on results obtained in a previous investigation (Ref. 5) (with a heat input between 5.2 and 8.0 kJ/mm), as well as relevant literature data (Refs. 6–13), a primary weld metal acicular ferrite volume fraction of approximately 50% may give rise to a 35 J (26 ft-lb) impact transition temperature well below –40°C (–40°F).

Application of high heat input in welding of offshore structures requires, however, information on fracture toughness properties. The present investigation was undertaken with the objective to examine the crack tip opening displacement (CTOD) fracture toughness of procedure test welds using submerged arc welding with both solid and flux cored welding wire, as well as submerged arc welding with iron powder additions (solid wire). Included were nondestructive evaluation and side bend testing, together with hardness measurements, Charpy V-notch and tensile testing. It is shown that high impact and fracture toughness may be obtained in the weld metal, both in the as-welded condition and after postweld heat treatment (PWHT).

KEY WORDS

Offshore Structures
Microstructure
High Heat Input Welding
PWHT
Welding Procedures
Weld Metal Properties
SAW
Titanium Content
FCAW
Mechanical Properties

Materials and Experimental Procedure

Materials and Welding

For the present investigation, five different welding consumables were selected. Included were three different commercially available welding consumables and two consumables that represent various modifications (one high in titanium, and one high in boron). All welds were deposited in double V-grooves on 60-mm (2.4-in.) thick base plates corresponding to Statoil Grade 1, with chemical composition guidelines outlined in Table 1. The weld test assembly is shown in Fig. 1, and reveals that 4000-mm (13.12-ft) long welds were deposited with a root opening of 2 mm (0.008 in.) and a bevel angle of either 40 or 50 deg. The applied welding parameters are summarized in Table 2. These were adjusted to give heat inputs of 3, 5 and 7 kJ/mm (76, 127 and 178 kJ/in.). Typical macrographs are shown in Fig. 2 for both low and high heat in-

G. RØRVIK, M. I. ONSØIEN, A. O. KLUKEN and O. M. AKSELSEN are with The Welding Center — SINTEF, The Foundation for Scientific and Industrial Research at the Norwegian Institute of Technology, Trondheim, Norway.

Table 1—Chemical Composition Guidelines for Statoil Grade 1[(a)] (Elements in wt-%).

C	Si	Mn	P	S	Cu	Ni	Cr	Mo	V	Nb	Ti	Al
0.12	0.45	1.60	0.010	0.005	0.30	0.70	0.20	0.08	0.006	0.03	0.03	0.05

(a) Minimum 325 MPa yield strength for 60-mm plate thickness.

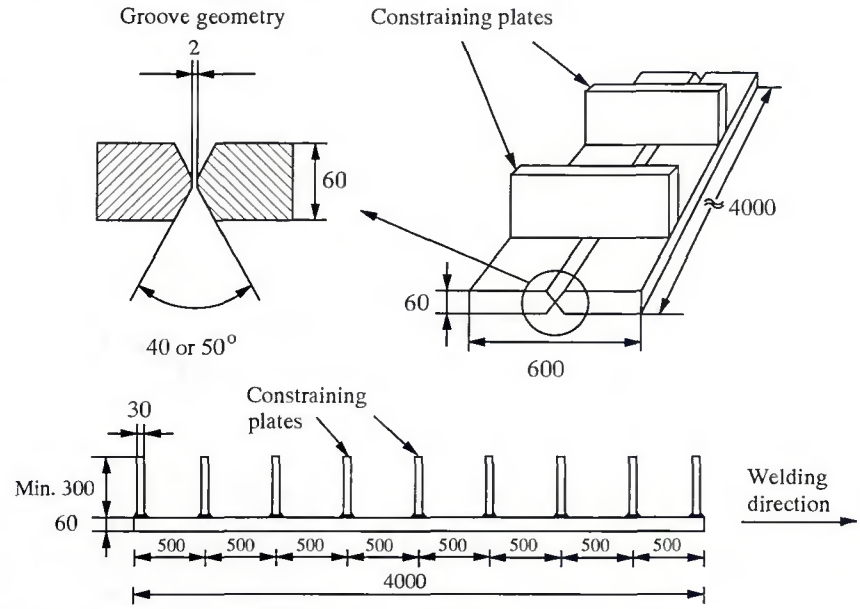

Fig. 1 — Weld test assembly (dimensions in mm).

Table 2—Welding Parameters (Fill Passes).

Weld No.	Wire	Diameter (mm)	Flux	Metal Powder	Current I (A)	Voltage U (V)	Travel Speed (mm/s)	Heat Input E (kJ/mm)	Groove Angle (deg)
A	OK 13.27[a]	4.0	OK 10.62	OK 21.86	700-750	32-34	4.7-5.8	5	50
B	OK 13.27[a]	4.0	OK 10.62	None	700-725	32-35	3.3	7	50
C	LAC Ni2[b]	2.4[c]	980	None	450-500	34-37	3.3-3.8	5	40
D	LAC Ni2[b]	2.4[c]	980	None	500-525	37	2.8	7	50
E	SD3[a]	4.0	OP121TT	PD3NiMo	700-750	33	7.5-8.3	3	50
F	SD3[a]	4.0	OP121TT	PD3NiMo	750	33	5.0	5	50
G	NW2[b]	4.0	P 240	None	800	32	3.6	7	40
H	NW2[b]	4.0	P 240	None	820	31	3.6	7	50
I	OK 13.27[a]	4.0	OK 10.62	OK 21.86	650-700	26-29	5.8-6.7	3	50
J	OK 13.27[a]	4.0	OK 10.62	OK 21.86	780	33	5.0	5	50
K	NW 10[b]	4.0	P 240	None	800	31	5.0	5	40
L	NW 10[b]	4.0	P 240	None	850	32	3.8	7	40

a. Solid wire.
b. Flux cored wire (NW2 and NW10 represent various modifications of the commercial Coreweld 70 wire).
c. 3/32 in.

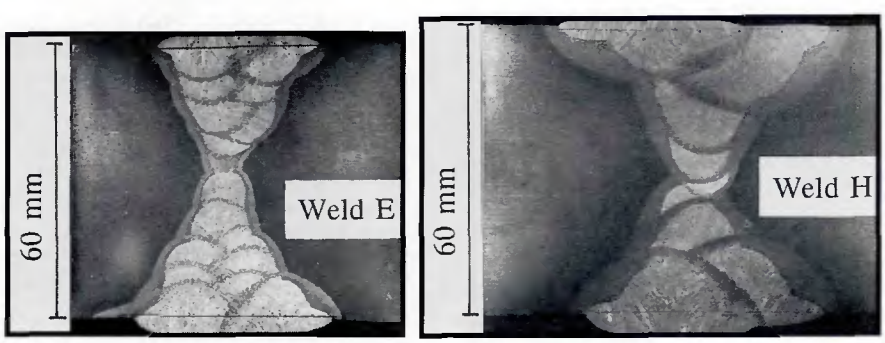

Fig. 2 — Example of weld macrograph. Left — Weld E; right — Weld H.

puts. The preheating and interpass temperatures were 50° and 250°C (122° and 484°F), respectively. The root bead and buffer layers were deposited with a 1.2 mm (0.045 in.) 80Ni- 1 flux cored wire using 75% Ar/25% CO_2 shielding gas, and a heat input of 1.7 kJ/mm (43 kJ/in.). In the case of submerged arc welding with iron powder additions, powder amounts of maximum 9 kg/h (20 lb/h) were added. One half of the procedure welds (2000-mm length) was subjected to PWHT at 600°C (1112°F) for 2 ½ h to obtain information on the potential effects of PWHT on weld metal hardness, tensile strength and ductility, as well as impact and fracture toughness.

Testing

All nondestructive evaluation (NDE), side bend and mechanical testing were performed in conformance with the Statoil Gullfaks C specification (CO17-A-N-SP-304). The nondestructive examination included ultrasonic and magnetic particle inspection.

The side bend test dimensions were 300 X 60 X 10 mm (12 X 2.4 X 0.4 in.), with a former diameter of 30 mm (1.2 in.) and a 180-deg bending angle. Two parallel tests were carried out for each wire/flux combination.

The room-temperature tensile properties and Charpy V-notch (CVN) toughness at –40°C were assessed for all welds, with specimens machined from the welds as schematically illustrated in Fig. 3. The tensile test specimens machined from fill passes were of 100-mm (4-in.) length (50-mm gauge length) with a diameter of either 6 or 8 mm (0.24 or 0.31 in.). Impact properties, based on the ASTM Charpy V-notch specimen dimensions of 10 X 10 X 55 mm (0.4 X 0.4 X 2.2 in.), were examined in both the root region and the fill passes, with three parallel tests for each position.

Machining of B X 2B specimens and CTOD testing were carried out in agreement with the British Standard BS 5762:1979, which includes preparation of the notch and fatigue precracking (this is similar to ASTM Standard 1290-89,1989, *Standard Test Methods for Crack Tip Opening Displacement (CTOD) Fracture Toughness Measurements*). The location of CTOD specimens is shown in Fig. 4 (*i.e.*, crack propagation through the weld metal). Three parallel tests were run at –10°C (14°F) for each wire/flux combination.

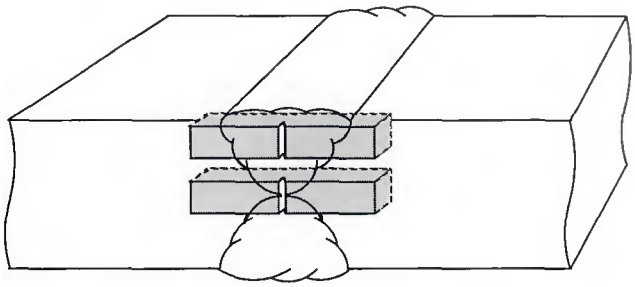

Fig. 3 — Location of CVN specimens (schematic).

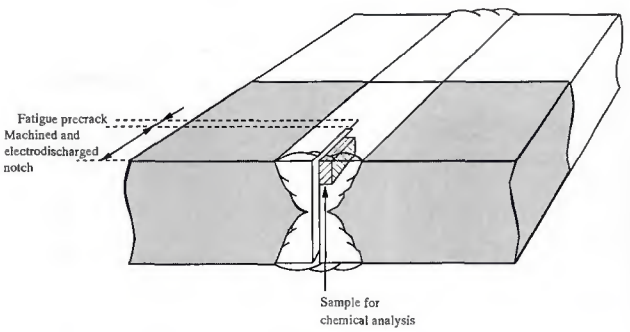

Fig. 4 — Location of CTOD specimens (schematic).

Chemical Analysis

The weld metal chemical composition was determined by emission spectroscopy with exception of elements such as carbon, sulfur, nitrogen and oxygen, which were analyzed with a Leco machine. The specimens were machined from CTOD test plates as shown schematically in Fig. 4.

Metallography

The metallographic examination was performed to determine the location of brittle fracture initiation (*i.e.*, primary or reheated weld metal). Specimens were cut from CTOD assemblies (low CTOD values only) and sectioned in agreement with Fig. 5, and subsequently prepared by standard metallographic techniques (grinding, polishing and etching). The brittle fracture initiation area was examined in a JEOL JSM-840 scanning electron microscope (SEM). Thin foils were prepared for a closer examination of the microstructure in a JEOL 200 CX transmission electron microscope (TEM). Included in the metallographic examination are also hardness measurements (HV_{10}, *i.e.*, 10-kg load) taken 1 mm (0.4 in.) below the plate surface on specimens cut perpendicular to the welding direction. Examples of hardness traverses are shown in Fig. 2.

Table 3—Typical Deposition Rates.

Weld No.	Welding Technique	Heat Input E (kJ/mm)	Deposition Rate (kg/h)
I	SAW/IP[a]	3	15
J	SAW/IP[a]	5	18
K	SFCAW[b]	5	13
L	SFCAW[b]	7	18

a. Submerged arc welding with iron powder additions.
b. Submerged flux cored arc welding.

Results and Discussion

Procedure Welding

In general, welding with high heat input was performed without technical problems, with a few exceptions of magnetic blow. Poor slag detachment has been found in the case of a bevel angle of 40 deg (Welds C and G), which means that high heat input welding may require a bevel angle of minimum 50 deg. However, this does not necessarily give rise to an increase in the total welding time. This is due to the fact that very high deposition rates have been obtained, as shown by the data contained in Table 3. Conventional submerged arc welding with 3 kJ/mm results in a deposition rate of typically 7 to 8 kg/h (15 to 18 lb/h). This level can be raised to 18 kg/h (40 lb/h) in the case of submerged arc welding with a flux cored wire using 7 kJ/mm heat input, or conventional submerged arc welding with a solid wire and iron powder additions using an arc energy of 5 kJ/mm.

Thus, high heat input welding may give rise to a substantial enhancement of the deposition rate (*i.e.*, 150%). This provides a basis for increased productivity. It follows that the productivity potential involved in high heat input increases with increasing plate thickness.

NDE and Side Bend Test Results

Both the magnetic particle and the ultrasonic inspection revealed only a few cases of undercuts and incomplete fusion in the root region. However, all welds were acceptable with respect to the current specification requirements. The side bend test results were also acceptable, both in the as-welded condition and after PWHT.

Weld Metal Chemical Composition

The chemical composition of welds A through L are outlined in Table 4. An inspection of the table reveals that the weld metal carbon content is similar between the consumables (0.06–0.08% C).

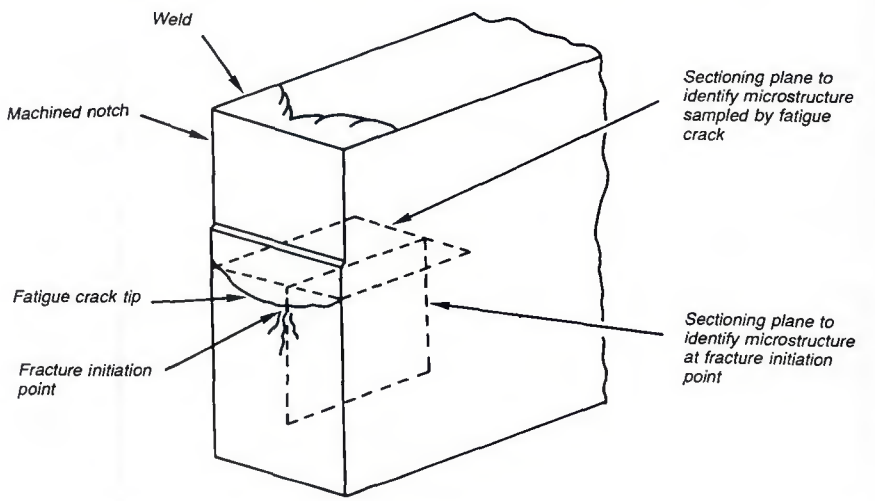

Fig. 5 — Sectioning of CTOD specimens for determination of brittle fracture initiation (schematic).

Table 4—Weld Metal Chemical Composition (Elements in wt-%)[a]

Weld No.	C	Si	Mn	P[b]	S[b]	N[b]	Ni	Al	Cu	Nb[b]	Ti[b]	B[b]	O	P_{cm}[c]
A	0.07	0.34	1.23	100	50	60	1.64	0.011	0.13	70	50	12	0.031	0.185
B	0.07	0.35	1.24	120	50	70	1.67	0.011	0.15	60	50	12	0.026	0.188
C	0.06	0.26	1.54	120	60	40	1.89	0.030	0.05	80	170	12	0.032	0.188
D	0.06	0.26	1.61	140	60	30	1.97	0.026	0.08	80	120	11	0.030	0.195
E[d]	0.06	0.33	1.32	130	60	60	0.90	0.011	0.10	100	30	6	0.027	0.173
F[e]	0.07	0.29	1.29	140	60	60	0.69	0.010	0.07	70	30	4	0.030	0.174
G	0.07	0.55	1.84	140	100	40	0.15	0.020	0.05	70	230	9	0.025	0.195
H	0.07	0.55	1.90	150	90	40	0.11	0.020	0.06	90	210	8	0.023	0.197
I	0.06	0.29	1.13	80	50	70	1.80	0.011	0.07	30	50	11	0.033	0.169
J	0.06	0.28	1.14	80	40	60	1.07	0.012	0.08	30	50	10	0.032	0.167
K	0.07	0.44	1.83	120	120	40	0.19	0.021	0.05	30	70	34	0.040	0.204
L	0.08	0.43	1.87	140	110	40	0.15	0.018	0.05	30	50	31	0.033	0.213

a. All welds contain 0.03–0.05%Cr.
b. Elements in ppm.
c. P_{cm} = C + Si/30 + (Mn + Cr + Cu)/20 + V/10 + Mo/15 + Ni/60 + 5B.
d. With 0.16%Mo.
e. With 0.14%Mo.

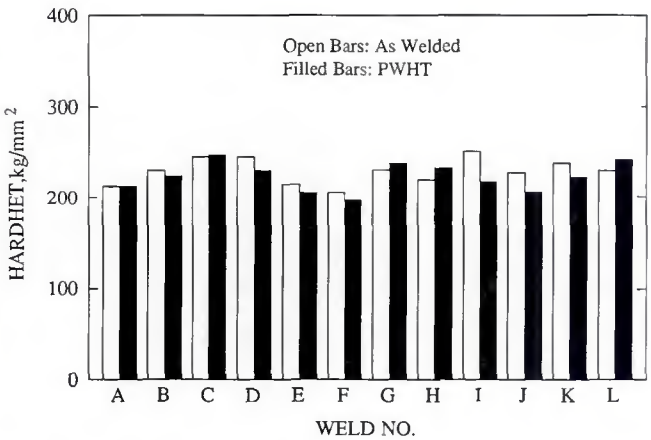

Fig. 6 — Weld metal hardness.

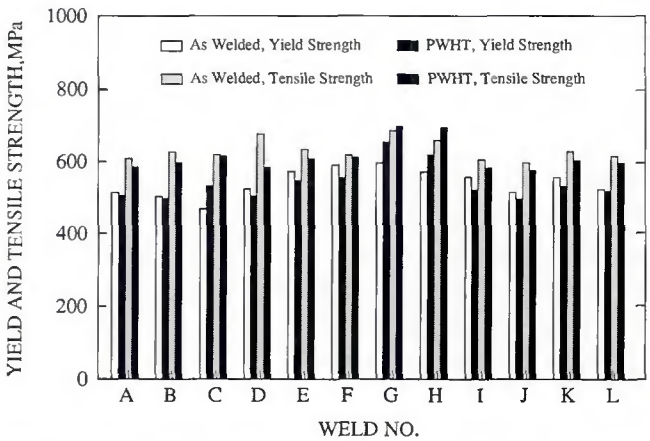

Fig. 7 — Weld metal yield and tensile strength.

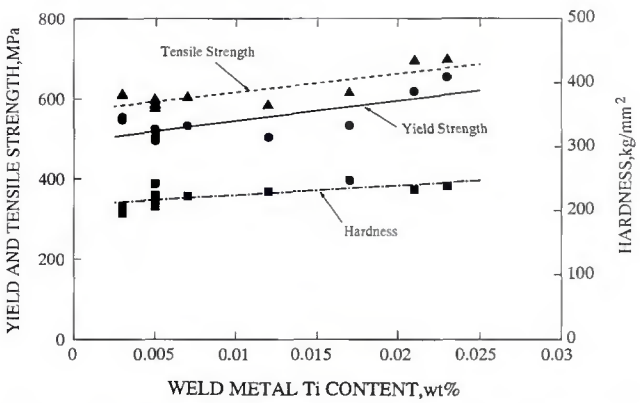

Fig. 8 — Effect of weld metal titanium content on yield and tensile strength after PWHT.

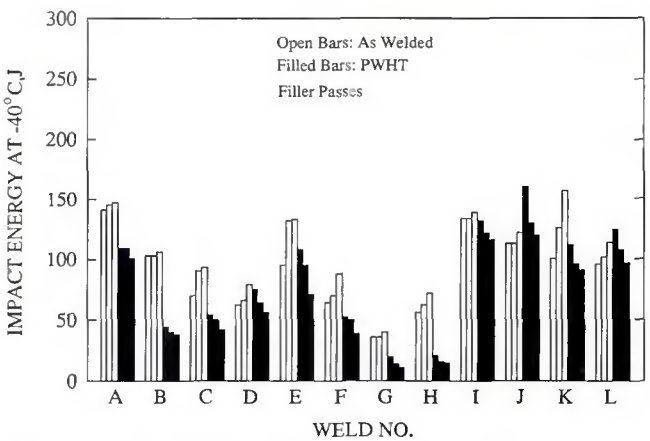

Fig. 9 — Weld metal CVN toughness at –40°C (fill passes).

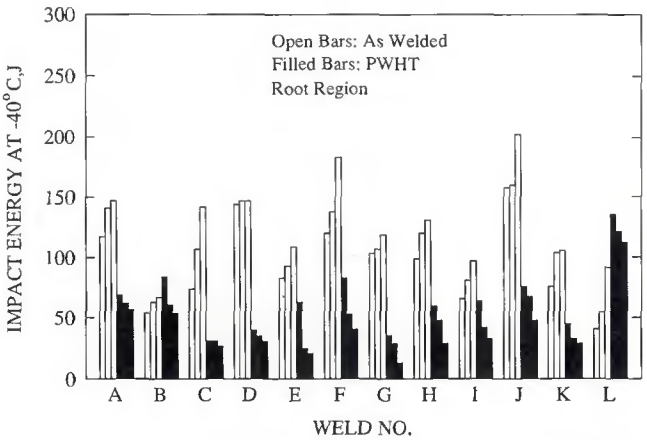

Fig. 10 — Weld metal CVN toughness at –40°C (root region).

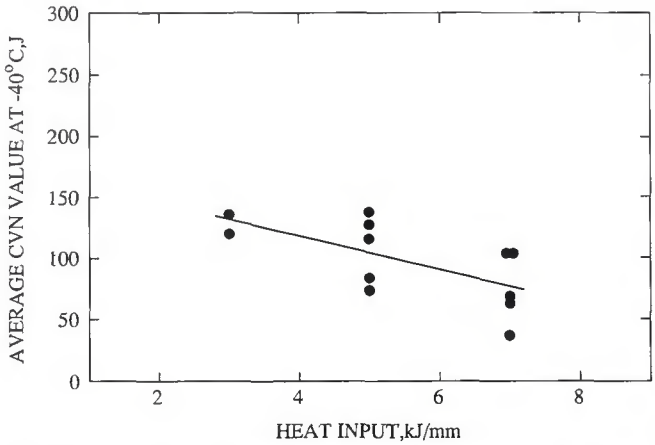

Fig. 11 – Effect of weld heat input on CVN toughness at –40°C, as-welded (fill passes).

A low nitrogen level was also found (0.004–0.007%N). However, the alloying level is different (P_{cm} values between 0.167 and 0.213), with variation in manganese from 1.13 to 1.90% and nickel from 0.11 to 1.97%. In addition, the concentration of microalloying elements is different, represented by a high titanium level in Welds C, G and H (0.017–0.023%Ti), and a high boron content in welds K and L (> 30 ppm). Note also the variations in the weld metal aluminum and oxygen contents, which together with silicon, manganese and titanium may influence the resulting transformation behavior through their influence on deoxidation and subsequent solidification grain structure (Refs. 14–16).

Weld Metal Hardness, Strength and Ductility

The data obtained from hardness measurements (HV_{10}) are outlined in Table 5 and presented graphically in Fig. 6. It is seen from the table that low hardness values were found, *i.e.*, HV_{10} within the range from 206 to 251 kg/mm^2 in the as-welded condition, and from 197 to 247 kg/mm^2 after PWHT. This observation is not surprising, considering the slow cooling rates involved in high heat input welding (the cooling time between 800° and 500 °C is typically 30 to 70 s). In general, PWHT gave rise to a small reduction of the weld metal hardness. An exception was found for the titanium-containing welds G and H.

In contrast to the low hardness level, relatively high yield and tensile strength values have been obtained — Table 5. This point is illustrated in Fig. 7. PWHT resulted in a reduction of the weld metal strength, with an exception for Welds C, G and H, where the yield strength was raised by 50 to 65 MPa (7252–9427 lb/in.^{2}). Also, the tensile strength level was increased for the two titanium-containing welds G and H by 12 to 35 MPa (1740–5076 lb/in.^{2}), but to a smaller extent than the yield strength. It is reasonable to suggest that these results are caused by the high titanium content, providing conditions for secondary hardening as a result of particle precipitation. Thus, it is not surprising that both the hardness and the strength level after PWHT are closely related to the weld metal Ti content, as shown by Fig. 8. In contrast, when considering the variations in the weld metal concentration of alloying elements (P_{cm} values ranging from 0.167 to 0.213), no straightforward relationship between alloying level and yield or tensile strength was found.

The tensile ductility was relatively high, represented by elongation at fracture (50-mm gauge length) within the range from 16 to 28% in the as-welded condition, and between 18 and 28% after PWHT —Table 5.

Weld Metal Impact Properties

The CVN test results are summarized in Table 6, and presented graphically in the form of vertical bars in Figs. 9 (fill passes) and 10 (root region). It is apparent from Fig. 9 that the notch toughness

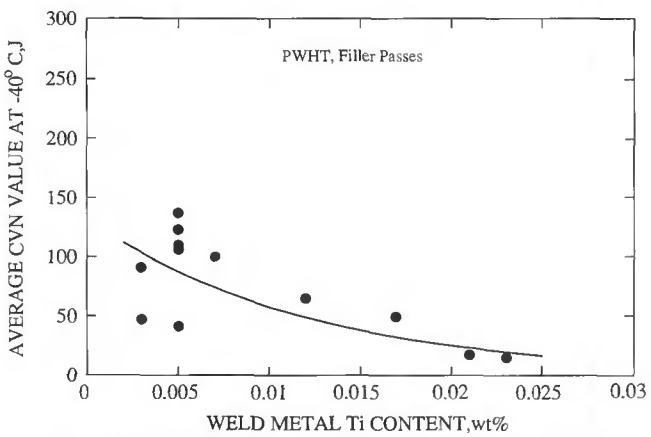

Fig. 12 — Effect of weld metal titanium content on CVN toughness at –40°C, PWHT (fill passes).

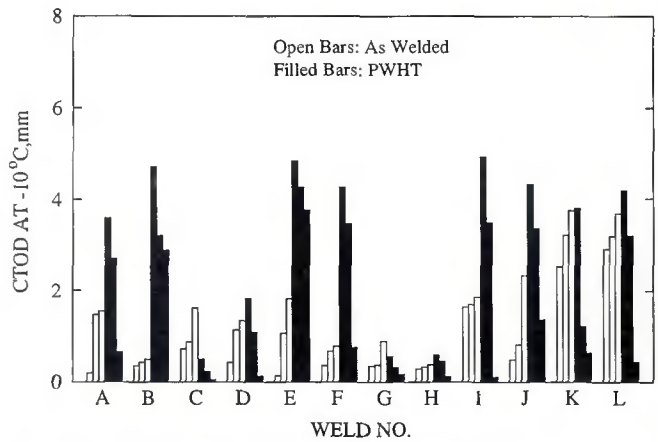

Fig. 13 — Weld metal CTOD fracture toughness at –10°C.

Table 5—Weld Metal Hardness, Strength and Ductility

Weld No.	As-Welded Condition				PWHT			
	HV_{10kg} (kg/mm²)	$\sigma_{p0.2}$ (MPa)	σ_m (MPa)	Elongation (%)	HV_{10kg} (kg/mm²)	$\sigma_{p0.2}$ (MPa)	σ_m (MPa)	Elongation (%)
A	213	515	609	17	213	505	586	18
B	230	503	627	16	224	497	598	20
C	245	468	619	28	247	533	615	26
D	245	526	676	21	230	504	584	25
E	215	574	635	23	206	548	609	23
F	206	591	618	26	197	555	612	24
G	231	596	685	21	238	654	697	21
H	220	572	659	24	233	619	694	24
I	251	558	606	25	218	524	583	28
J	228	516	597	27	207	495	576	28
K	238	557	628	28	223	533	604	27
L	230	525	616	27	242	519	596	27

of fill passes is high in the as-welded condition, between 50 and 150 J (37 and 111 ft-lb). An exception is found for Weld G (0.023% Ti), where the CVN values approach 35 J (26 ft-lb). A closer inspection of the CVN data shows that the toughness is dependent on the weld heat input, as shown by Fig. 11. This is not surprising since an increase in the heat input results in a general coarsening of the microstructure.

In general, PWHT gave rise to a deterioration of the CVN toughness, particularly in the root region (Fig. 10). In the case of Welds G and H, the impact energy of filler passes falls below 27 J (20 ft-lb) subsequent to PWHT. This loss in notch toughness is probably associated with an increase in the strength level. Hence, it would be expected that the impact energy is dependent on the weld metal's titanium content, as experienced with the strength data. An illustration of this point is contained in Fig. 12. In spite of the high heat input applied, welds A (51 kJ/mm), B (7 kJ/mm), F (5 kJ/mm), I(3 kJ/mm), J (5 kJ/mm) and L (7 kJ/mm) appear with CVN levels above 35 J. Presupposed that the 27-J limit is required, only Welds E, G and H reveal insufficient impact properties in the PWHT condition. Note that weld E has an average CVN value of 36 J, which indicates that small changes in the welding procedure may give rise to satisfactory CVN toughness.

Weld Metal Fracture Toughness

The results from CTOD testing at –10°C are outlined in Table 6, and presented graphically in Fig. 13. In the as-welded condition, very high CTOD values were obtained (above 0.2 mm). The CTOD level seems to decrease with increasing heat input, as shown by the data plotted in Fig. 14. A closer inspection of Figs. 13 and 14 reveals a very high fracture toughness for the two boron-containing Welds K and L (CTOD > 2.5 mm).

The CTOD level is further enhanced by PWHT. This would be expected if the fracture toughness improvement is controlled by relaxation of weld residual stresses. However, a loss in fracture toughness was found for the welds with high titanium (Welds C, D, G and H) or boron contents (Welds K and L). Note that the latter two welds still possess a high CTOD level (> 1.8 mm). In the case of Welds C, G and H, the reduction in the CTOD level is probably associated with the increase in yield strength as a result of precipitation hardening. As experienced with notch toughness, the CTOD values after PWHT was influenced by the weld metal titanium content, as shown by Fig. 15. This may imply that an embrittling mechanism is introduced during PWHT.

In summary, the CTOD data obtained both in the as-welded and the PWHT conditions are sufficiently high to satisfy current offshore specifications, with the exception of the low values occasionally found after PWHT.

Metallography

Previous examination of primary weld metal microstructures, based on high heat input welding with the consumables applied in the present investigation, showed that acicular ferrite was the predominant constituent (minimum 67%), balanced by small amounts of ferrite sideplates (< 5%) and grain boundary ferrite (typically 15–20%) (Refs. 17, 18). The two boron-containing welds possessed the lowest amount of grain boundary ferrite (< 15%), and the highest fraction of acicular ferrite (> 80%), which in fact is in close agreement with the excellent CVN and CTOD values. This observation is not surprising, considering the fact that boron may prohibit the formation of proeutectoid ferrite through segregation of free boron to austenite grain boundaries on cooling in a similar way as previously reported for heat-affected zones of low-carbon microalloyed steel (Ref. 9). Hence, the

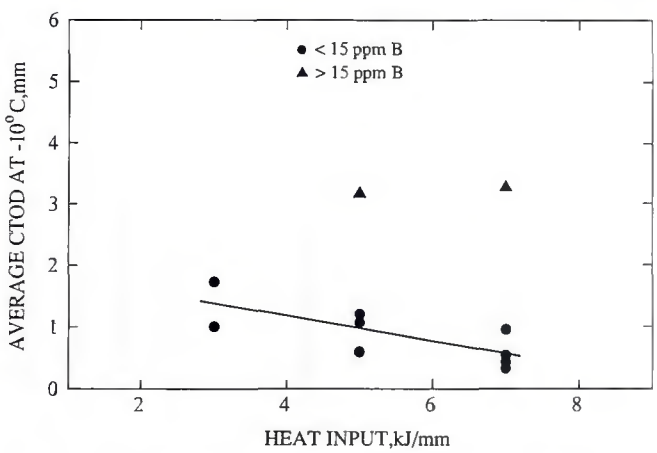

Fig. 14 — Effect of weld heat input on CTOD fracture toughness at –10°C, as-welded.

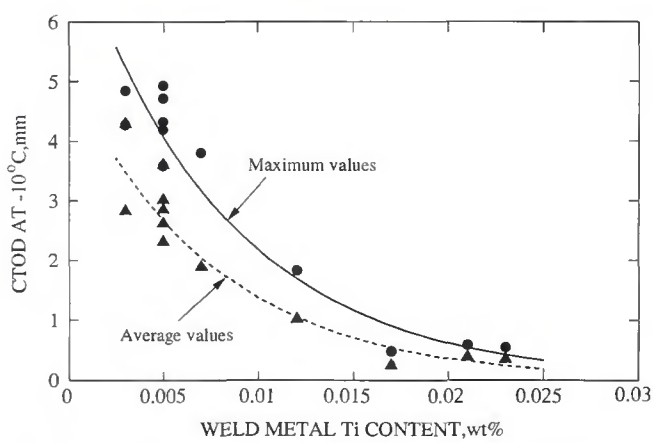

Fig. 15 — Effect of weld metal titanium content on CTOD fracture toughness at –10°C, PWHT.

Table 6—Weld Metal Impact (−40°C) and Fracture Toughness (−10°C).

Weld No.	As Welded Condition			PWHT		
	Energy Absorption (J)		CTOD, mm[a]	Energy Absorption (J)		CTOD, mm[a]
	Fill	Root		Fill	Root	
A	141-145-127	141-117-147	0.19c-1.47u-1.55u	101-109-109	57-69-62	3.59m-2.70m-0.65u
B	103-103-106	63-67-54	0.36c-0.49c-0.43c	38-44-40	54-61-84	2.89m-3.21m-4.72m
C	70-93-90	142-107-74	0.87m-0.72m-1.61m	42-54-50	31-31-27	0.49u-0.22c-0.05c
D	79-62-66	144-147-147	1.33m-0.42u-1.13u	75-56-64	35-40-31	1.83u-1.09u-0.13c
E	95-133-132	83-93-109	1.82u-0.14c-1.07u	95-71-108	21-25-63	4.27m-4.85m-3.77u
F	64-70-88	183-138-120	0.78u-0.67u-0.36c	50-52-39	83-41-53	4.27m-3.47m-0.75u
G	36-40-36	103-107-119	0.35c-0.89m-0.37c	14-20-11	36-29-13	0.17c-0.32c-0.55u
H	56-72-62	99-120-131	0.38c-0.29c-0.33c	21-16-15	60-29-48	0.12c-0.45c-0.59u
I	139-134-134	81-97-66	1.69m-1.63m-1.86m	132-122-116	33-64-42	3.50m-0.11c-4.94m
J	113-113-122	158-202-160	0.48u-0.81u-2.33m	120-130-160	68-48-76	3.37u-4.33m-1.36u
K	126-101-157	106-76-104	3.22m-3.76m-2.52m	112-91-96	45-33-29	1.22u-0.65u-3.81m
L	96-102-114	55-92-41	3.20m-2.91m-3.69m	97-108-125	122-136-113	4.20m-3.21u-0.44c

a. Nomenclature in agreement with British Standard BS 5762:1979.

present investigation, together with previous findings (Ref. 5), may imply that the formation of acicular ferrite becomes nearly independent of the weld cooling time, provided a sufficient hardenability to prevent an excessive formation of proeutectiod ferrite. Consequently, excellent weld metal properties may be obtained, even in the case of high heat input welding.

From a metallurgical standpoint, it would be expected that initiation of brittle fracture occurs at microstructural sites with a low intrinsic cleavage resistance. In fact, such sites are present as follows: 1) the grain refined or the intercritically reheated region in the form of a low volume fraction of very small martensite-austenite (MA) islands, presumably with a local carbon concentration of minimum 0.5 to 0.6% C; and 2) classic temper embrittlement for PWHT specimens, revealed by intergranular fracture. In the former case, it was verified previously that martensite-austenite islands, consisting of both lath and plate martensite, may give rise to a considerable loss in toughness, based on both CVN (Refs. 20, 21) and CTOD testing (Ref. 22). Hence, the initiation presumably starts at the interface between a hard particle (M-A, high yield strength) and a soft matrix (polygonal ferrite, low yield strength) due to the high transformation stresses developed at the ferrite/M-A interface exceeding the cleavage strength of ferrite. It should be noted that the microhardness (10-g load) of these islands exceeded 400 kg/mm^2 in the as-welded condition, and above 300 kg/mm^2 after PWHT at 600°C for 2½ h. The formation of M-A islands is promoted by a high manganese content (Welds G, H, K and L) or a combination of medium-manganese and high-nickel content (*e.g.*, Welds A, B, C, D and I). In addition, small amounts of boron may increase the hardenability of austenite islands considerably (Ref. 23). It appears that about 6 vol-% of the M-A constituent is required to cause a significant loss in the heat-affected-zone CVN toughness. A similar critical amount would be expected in the weld metal, provided that the ferrite grain size is similar (a refinement of the grain structure will presumably result in a higher critical M-A volume fraction).

The metallographic examination carried out for CTOD specimens with low values revealed that brittle fracture initiation occurred preferentially within the grain refined or the intercritically reheated region rather than within the primary weld metal. Moreover, in most cases (Welds C, D, H and I), the initiation was found to take place within or close to the root region, particularly when the root bead deposited with the 80Ni-1 flux cored wire was not fully remelted. This may imply that the selection of consumables for deposition of

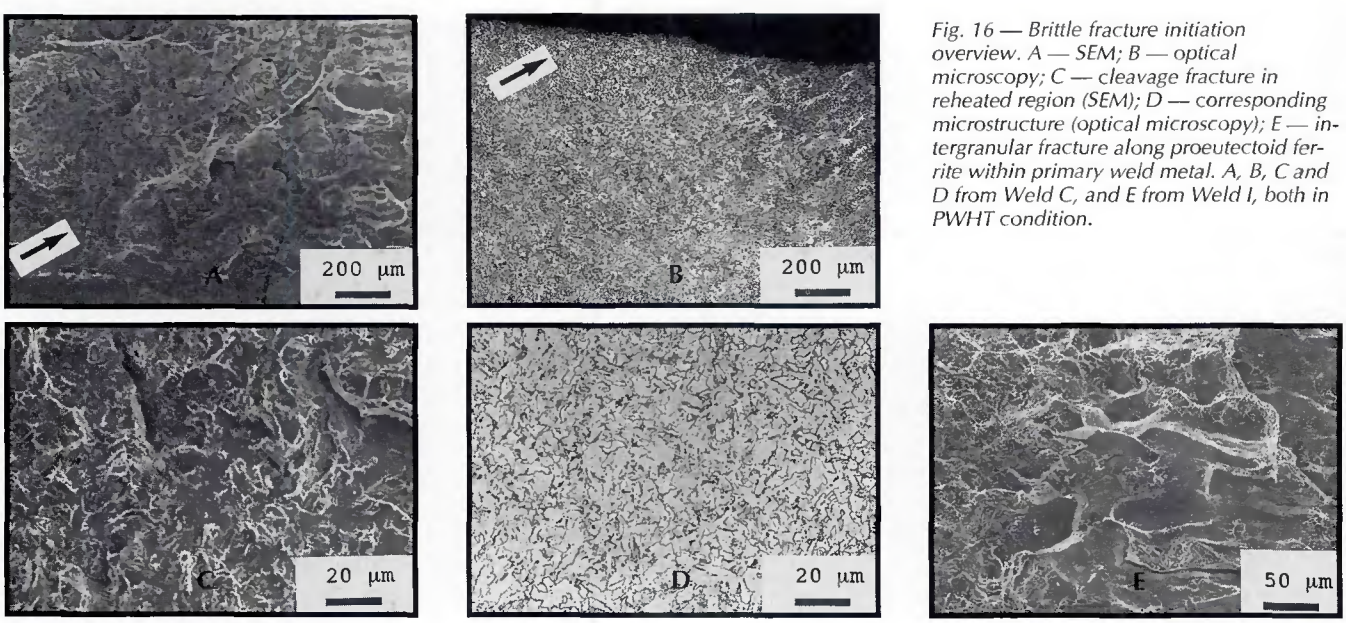

Fig. 16 — Brittle fracture initiation overview. A — SEM; B — optical microscopy; C — cleavage fracture in reheated region (SEM); D — corresponding microstructure (optical microscopy); E — intergranular fracture along proeutectoid ferrite within primary weld metal. A, B, C and D from Weld C, and E from Weld I, both in PWHT condition.

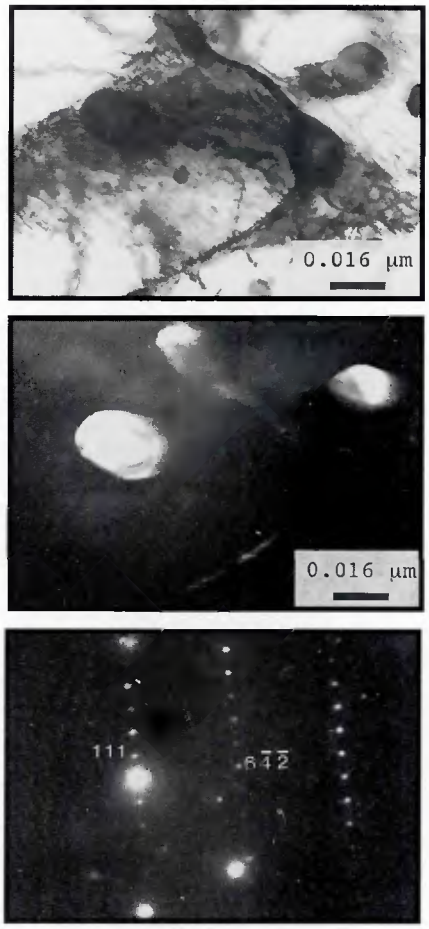

Fig. 17 — TEM micrograph of grain boundary iron borocarbides in weld C, $F_{23}(B,C)_6$. Top to bottom: Bright field image, corresponding dark field image, diffraction pattern. Thin foil taken from the fracture initiation area of the CTOD specimen with the lowest value (0.05 mm).

root pass and buffer layers is important. It is recommended that these consumables should be metallurgically compatible with those applied in deposition of fill passes when it comes to chemical composition, resulting solidification microstructure, as well as nonmetallic inclusion number density and size distribution. An example of brittle fracture initiation within the grain-refined reheated region is illustrated in Fig. 16 for Weld C. The initiation area is indicated by arrows (Fig. 16A and B). It is seen from the fractograph in Fig. 16C that the fracture mode is mainly transgranular cleavage. The corresponding microstructure is shown in Fig. 16D, resembling predominantly polygonal ferrite with a fine grain size. In addition, the SEM examination revealed intergranular fracture within the primary weld metal of fill passes, *i.e.*, fracture occurred along the coarse grain boundary ferrite. An example is shown for weld I in Fig. 16E. The presence of an intergranular fracture appearance requires that the following conditions are met (Refs. 24, 25).

1) Strengthening of matrix, *i.e.*, precipitation of second-phase particles. In the present investigation, it would be expected that titanium nitride was formed due to the observed effect of Ti on the weld metal strength level after PWHT. Such small semicoherent or coherent particles are not easily identified through TEM examination due to complex diffraction patterns.

2) Particles present at grain boundaries acting as stress concentrators. These are borocarbides of the type $Fe_{23}(B, C)_6$, as shown by the TEM micrographs in Fig. 17. The formation of borocarbides may take place even when only a few ppm boron is present due to the strong segregation ability of boron atoms.

3) Weakening of grain boundaries through impurity segregation, *i.e.*, phosphorus. Note that the phosphorus content is higher than that specified as an upper limit in modern structural steels (maximum 0.01% P). Here, the weld metal solidification pattern is important, since it may influence the extent of phosphorus segregation (Ref. 15). This, in turn, may affect the segregation of boron atoms since less grain boundary sites are available after extensive phosphorus segregation.

Based on the SEM observations, both embrittling mechanisms described above are probably operating. However, with the exception of the low value of 0.05 mm for Weld C, the CTOD values are still at a very high level, and satisfy the requirements set in many offshore specifications. On the other hand, further work is still necessary to establish a better understanding of the metallurgical phenomena controlling the microstructure-property relationships in welding of titanium and boron-containing consumables.

Practical Implications

From the present investigation, the weld metal properties established imply that high heat input welding may be applied in fabrication of offshore structures when welding in the 1G position is possible. For many years, it has been argued that the heat-affected zone developed under such conditions may give rise to a low cleavage resistance. At present, however, results available from testing laboratory heats of modern structural steels indicate that they may tolerate high heat inputs (Refs. 3, 4). Recent observations made from CTOD testing of single bead in groove weldments (with a heat input of 4 kJ/mm) show that high HAZ fracture toughness may be obtained, provided that the base plate phosphorus content is kept below 0.01% P (Ref. 26, 27). High CTOD values were also found through thickness testing of commercially available structural steels, based on the frequently used K-groove type because of the reasonably straight fusion line obtained, facilitating assessment of the grain-coarsened HAZ cleavage resistance (Refs. 28, 29).

In the present investigation, a few CVN specimens were machined from HAZ with the notch located at the fusion line (FL), together with the FL+2 mm and FL+5 mm positions. The results from testing at −40°C are summarized in Table 7. The average of three parallel tests were minimum 46 J (34 ft-lb) for all welds, with the exception of Weld A in both the as-welded and PWHT condition and Weld D after PWHT. These re-

Table 7. Heat-Affected Zone CVN Toughness at −40°C.

	As-Welded CVN Toughness at −40°C (J)			CVN Toughness at −40°C after PWHT (J)		
Weld No.	Fusion Line	Fusion Line +2 mm	Fusion Line +5 mm	Fusion Line	Fusion Line +2 mm	Fusion Line +5 mm
A	26-59-100	28-24-38	84-76-100	31-96-22	28-47-41	147-147-147
B	83-65-45	59-51-43	93-82-84	144-89-80	56-147-40	110-147-109
C	49-38-72	64-71-47	147-147-44	57-35-32	64-59-87	93-94-89
D	65-66-132	49-43-45	57-83-53	33-23-27	34-23-31	147-147-74
I	139-211-173	—	—	148-222-218	—	—
J	260-110-192	—	—	160-178-198	—	—
K	175-184-182	—	—	155-186-180	—	—
L	184-98-199	—	—	180-175-250	—	—

sults may imply that the HAZ formed under high heat input conditions possesses sufficiently high notch toughness, particularly when considering the fact that a level of 35 J is required at –40°C for the base plate strength and plate thickness employed in the present investigation, and that the selected base metal was not developed for high heat input welding. Further improvement of the heat-affected zone CVN toughness would therefore be expected when welding steels primarily developed to tolerate such extreme conditions.

Conclusions

The main conclusions are as follows:

1) Welding with high heat input did not result in technical problems, with the exception of a few cases of magnetic arc blow. Compared with conventional submerged arc welding with 3 kJ/mm, a substantial enhancement of the deposition rate was found when using iron powder additions or submerged flux cored arc welding with high heat input.

2) Satisfactory NDE and sidebend test results were obtained.

3) Relatively high weld metal strength values were found in the as-welded condition with yield and tensile strength within the range of 450 to 600 MPa (62.3–87 ksi) and 600 to 685 MPa (87–99.3 ksi), respectively. This level was further raised after PWHT for welds with a high titanium content (50 to 65 MPa increase in yield strength).

4) In general, excellent CVN and CTOD results were obtained in the as-welded condition, with a slight reduction with increasing heat input. PWHT gave rise to a deterioration in the CVN values, the extent of which was found to be dependent on the weld metal titanium content. A similar dependence was found for fracture toughness.

5) In general, the present investigation shows that the weld metal properties are not a limiting factor for applying high heat input in welding of offshore structures. This may provide a basis for an increased productivity.

Acknowledgments

The authors wish to thank B. Sørenes (Aker Stord), A. O. Back (Kvaerner Rosenberg) and P. O. Helden (Aker Verdal) for conducting the procedure test welding, NDE and sidebend testing, as well as hardness measurements. Thanks are also due to A. Brøsholen (Norweld), R. Jægersen (Sveiseindustri), S. Tandberg (ESAB), O. Bakke (Oerlikon) and L. Holmsen (Filarc) for their kind cooperation and provision of welding consumables. Finally, the financial support from the National Welding Program, NSP (Contract No. VK 36.0122790) is gratefully acknowledged.

References

1. Abson, D. J., Dolby, R. E., and Hart, P. H. M. 1978. Proc. Int. Conf. Trends in Steels and Consumables. London, Paper 25, The Welding Institute, Abington, England.

2. Grong, Ø., and Matlock, D. K. 1986. Int. Met. Rev. 31, p. 27.

3. Homma, H., Okita, S., Matsuda, S., and Yamamoto, K.1987. Improvement of HAZ toughness in HSLA steel by introducing finely dispersed Ti-Oxide. *Welding Journal* 66(10):301-s.

4. Yamamoto, K., Matsuda, S., Haze, T., Chijiiwa, R., and Mimura, H. 1987. Symp. Residual and Unspecified Elements in Steel. ASTM.

5. Kluken, A. O., Onsoien, M. I., Akselsen, O. M., and Rørvik, G. 1991. *Join. Sci.* 1, p. 14.

6. Bailey, N., and Pargeter, R. J. 1978. Weld. Inst. Rep. 70, Abington, England.

7. Bailey, N., and Pargeter, R. J. 1979. Weld. Inst. Report 101, Abington, England.

8. Terashima, H., and, Hart, P. H. M. 1982. The Welding Institute. Report 186, Abington, England.

9. Evans, G. M. 1982. The effect of heat input on microstructure and properties of C-Mn all-weld-metal deposits. *Welding Journal* 61(14):125-s.

10. Abson, D. J., and Evans, G. M. 1983. Proc. Int. Conf. The Effects of Residual, Impurity and Microalloying Elements on Weldability and Weld Properties. London, Paper 27. The Welding Institute, Abington, England.

11. Hemmer, H. 1986. Met. eng. thesis, The Norwegian Institute of Technology, Dept. of Metallurgy, Trondheim, Norway (in Norwegian).

12. Kluken, A. O., Grong, Ø., and Hemmer, H. 1987. SINTEF Report 5TF34 F87093, SINTEF, Trondheim, Norway.

13. Kluken, A. O., and Grong, Ø., and Hemmer, H. 1988. SINTEF Report STF34 F88040, SINTEF, Trondheim, Norway.

14. Kluken, A. O., and Grong, Ø., 1989. *Met. Trans.* 20A, p. 1335.

15. Kluken, A. O., Grong, Ø., and Rørvik, G. 1990. *Met. Trans.* 21A, p. 2047.

16. Kluken, A. O. 1990. Ph.D. thesis, The Norwegian Inst. of Technol., Dept. of Metal.

17. Kluken, A. O., Onsøien, M. I., Hemmer, H., and Akselsen, O. M. 1987. SINTEF Report 5TF34 A87140, (in Norwegian).

18. Onsøien, M. I., and Akselsen, O. M. 1988. SINTEF Report 5TF34 A881 18, (in Norwegian).

19. Akselsen, O. M., Grong, Ø., and Kvaale, P. E. 1986. *Met. Trans.* 17A, p. 1529.

20. Akselsen, O. M., Grong, Ø., and Solberg, J. K. 1987. *Mater. Sci.Technol.* 3, p. 649.

21. Akselsen, O. M., Solberg, J. K., and Grong, Ø. 1988. *Scand. J. Met.* 17, p. 194.

22 Chen, J. H., Kikuta, Y., Araki, T., Yoneda, M., and Matsuda, Y. 1984. *Acta Metall.* 32, p. 1779.

23. Ramberg, M., Akselsen, O. M., and Grong, Ø., 1986. Proc. Int. Conf. on Trends in Welding Research. Ed. S. A. David, ASM International, Materials Park, Ohio, p. 679.

24. Akselsen, O. M., Grong, Ø., and Rorvik, G. 1990. *Scand. J. Met.* 19, p. 258.

25. Kluken, A. O., and Grong, Ø. 1989. Unpublished research work, SINTEF.

26. Thaulow, C., Paauw, A. J., and Guttormsen, K. 1987. The heat-affected zone toughness of low-carbon microalloyed steel. *Welding Journal.* 66, p. 266-s.

27. Thaulow, C., and Paauw, A. J. 1988. Proc. Int. Conf. Weld Failures. Paper 24, The Welding Institute, Abington, England.

28. Lefebvre, G., and Denys, R. 1985. Proc. Conf. *Inclusions and Residuals in Steels: Effects on Fabrication and Service Behavior.* Eds. J. D. Boyd, C. S. Champion, Ottawa, Canada, p. 315.

29. Harneshaug, I. S., Vallan, G., Gundersen, K., and Roland, M. 1988. Proc. 7th Int.Conf. *Offshore Mechanics and Arctic Engineering.* Houston, Tex.

WRC Bulletin 339
December 1988

Development of Tightness Test Procedures for Gaskets in Elevated Temperature Service
By A. Bazergui and L. Marchand

In this report, different elevated temperature gasket tightness test procedures are compared. A two-tier test approach, involving aging of the preloaded gasket in a kiln followed by a short duration tightness test was evaluated. The procedures were evaluated using spiral-wound gaskets with two different fillers: a mica-graphite filler and an asbestos filler.

Publication of this report was sponsored by the Subcommittee on Bolted Flanged Connections of the Pressure Vessel Research Committee of the Welding Research Council. The price of WRC Bulletin 339 is $16.00 per copy, plus $5.00 for postage and handling. Orders should be sent with payment to the Welding Research Council, 345 E. 47th St., Suite 1301, New York, NY 10017.

WRC Bulletin 344
June 1989

This Bulletin contains two reports covering three-dimensional finite element analysis of 45-deg lateral branch pipe models.

(1) Three-Dimensional Finite Element Analysis of PVRC 45-Degree Lateral Model 4 ($d/D = 0.5$, $D/T = 40$) under Out-of-Plane Moment Loading on Branch Pipes
By P. P. Raju

(2) Three-Dimensional Finite Element Analysis of 45-Degree Lateral Model 2 ($d/D = 0.5$, $D/T = 10$) under Out-of-Plane Moment Loading on the Branch Pipe
By P. P. Raju

Publication of these reports was sponsored by the Joint Task Group on Laterals of the Subcommittee on Piping, Pumps and Valves, and the Subcommittee on Reinforced Openings of the Pressure Vessel Research Committee of the Welding Research Council. The price of WRC Bulletin 344 is $16.00 per copy, plus $5.00 for U.S., or $8.00 for overseas, postage and handling. Orders should be sent with payment to the Welding Research Council, 345 E. 47th St., Room 1301, New York, NY 10017.

WRC Bulletin 346
August 1989

WFI/PVRC Moment Fatigue Tests on 4 × 3 ANSI B16.9 Tees

By G. E. Woods and E. C. Rodabaugh

The Markl-type fatigue test data presented in this report have been needed for a number of years to establish i-factors (SIFs) for forged tees with d/D ratios between 0.5 and 1.0 that conform to the ANSI B16.9 standard. These new data will provide improved design rules for both nuclear and industrial piping systems.

Publication of this report was sponsored by the Subcommittee on Piping Pumps and Valves of the Pressure Vessel Research Committee of the Welding Research Council. The price of WRC Bulletin 346 is $25.00 per copy, plus $5.00 for U.S. and $10.00 for overseas postage and handling. Orders should be sent with payment to the Welding Research Council, Room 1301, 345 E. 47th St., New York, NY 10017.